Electrochimica Acta 55 (2010) 6885–6891

Contents lists available at ScienceDirect

Electrochimica Acta

journal homepage: www.elsevier.com/locate/electacta

Controlled synthesis and methanol sensing capabilities of Pt-incorporated ZnO nanospheres

Mashkoor Ahmad, Lin Gan, Caofeng Pan, Jing Zhu*

Beijing National Center for Electron Microscopy, The State Key Laboratory of New Ceramics and Fine Processing, Laboratory of Advanced Material, Department of Material Science and Engineering, Tsinghua University, Beijing 100084, China

ARTICLE INFO

Article history:
Received 21 March 2010
Received in revised form 17 May 2010
Accepted 25 May 2010
Available online 4 June 2010

Keywords:
ZnO
Platinum
Hybrid nanospheres
Methanol oxidation
Electrodeposition

ABSTRACT

Platinum nanoparticles incorporated ZnO hybrid nanospheres (PtZONS) have been synthesized via electrodeposition which is easy to control over the size distribution range. The Pt nanoparticles in ZnO nanospheres have been identified with high-resolution transmission electron microscopy (HRTEM) and energy dispersive spectroscopy (EDS). Methanol sensing capabilities of the nanospheres have been investigated through electrochemical measurements. The electrochemical measurements prove that these nanospheres demonstrate the abilities to electrocatalyze the oxidation of methanol and substantially raise the response current. The sensitivity of the Nafion/PtZONS/glassy carbon modified electrode to methanol is 235.47 $\mu A\,M^{-1}\,cm^{-2}$, which is much higher than that of a pure ZnO and Pt nanospheres modified electrodes. Furthermore, it has been revealed that the electrode exhibits a good anti-interference and long-term stability. Our investigation demonstrates that the Pt–ZnO nanospheres can be employed for various applications.

1. Introduction

Nanocrystal-based hybrid nanostructures have received great research attention because they may provide enhanced catalytic, photochemical/physical and thermal stability properties superior to a single system [1–3]. Furthermore, hybrid nanostructures are usually multifunctional [4,5]. Hybrid semiconducting nanostructures are currently a research focus owing to their potential in optoelectronics, drugs delivery, environmental monitoring, control of chemical processes and biomedical diagnosis applications [6,7]. These advantages make hybrid nanostructures one of the most promising candidates for the exploration of new applications. Among the noble metals, Platinum has found widespread use in a range of applications due to its unique physical and chemical properties [8–10]. It is also very attractive in that it can be introduced into ZnO lattice and is predicted to serve as a stable electron donor to the conduction band of ZnO [11]. Various methods have been developed for the synthesis of hybrid nanospheres with tunable size and controllable compositions [12,13]. Among different methods electrodeposition is considered an effective approach for the synthesis of hybrid nanostructures at room temperature with very simple and well-controlled manner. ZnO is a transparent oxide semiconductor that possesses piezoelectric properties, which has been widely used for solar cells [14], optoelectronics devices [15] and electromechanical coupled sensors and transducers [16]. Moreover, ZnO is biocompatible and can be directly used for biomedical applications [17,18]. However, it is well known to be difficult to grow the two materials together in a controlled manner due to lattice mismatch and a large difference in their surface free energies. In spite of many successful demonstrations, it remains a grand challenge to produce large quantities of noble metals-ZnO hybrid nanostructure, together with well-controlled dimensions and morphologies. Recently, many researchers have reported the inclusion of Pt into ZnO to enhance the electrocatalytic activity of the nanostructures, which is crucial for their practical applications (Ref. [11]). In our previous work, we have been successfully synthesized the PtZONS and repotted the highly sensitive amperometric cholesterol biosensor based on these nanospheres. It has been found that the combination of ZnO and Pt nanoparticles facilitates the low potential amperometric detection of cholesterol and enhances the anti-interference ability of the biosensor. Also, it has been revealed that ZnO improves the electrocatalytic activity of Pt nanoparticles, which in turn enhances the sensitivity of the biosensor for cholesterol detection [19].

On the other hand, methanol is one of the most widely used organic solvents, especially in industrial and household products. It is also potentially valuable as an alternative automobile fuel [20]. However, methanol exposure via inhalation and skin absorption may lead to toxic effects from headaches to blindness with

* Corresponding author. Fax: +86 10 62771160.
E-mail address: jzhu@mail.tsinghua.edu.cn (J. Zhu).

0013-4686/$ – see front matter © 2010 Elsevier Ltd. All rights reserved.
doi:10.1016/j.electacta.2010.05.075

direct digestion even leading to death [21]. Therefore, facile analysis procedures are important for monitoring methanol levels in the environment, in alcoholic beverages and for clinical diagnostic measurements. Methanol determination is also required in some biological processes. Many different instrumental methods are used for methanol determination, including GC-FID [22–24], HPLC with electrochemical [25], fluorescence [26] or UV–visible [27] detection and FTIR [28]. One simple alternative is an amperometric biosensor based on hybrid nanostructures, which works on the principle of raising current signal to recognize and oxidize methanol. The resulting current signal is then proportional to the methanol concentration and is useful for quantitation. The methanol electrooxidation is a very complex reaction because many intermediate species such as CO [29–31] and other carbonaceous species like HCO or COH [32–34] are involved. However, such reaction requires platinum-based catalysts, even though Pt exhibits a rather low activity [35]. The high activity of PtZONS in comparison with pure Pt would be expected to reduce the poisoning level due to influence of surface structure, providing low potential determination and net charge transfer. In this work, the focus of current study is divided into two parts; firstly, the controlled synthesis of PtZONS hybrid nanospheres, secondly, the fabrication of a methanol sensor based on PtZONS modified electrode. The performances of the sensor are characterized by electrochemical method that shows a good response.

2. Experimental

2.1. Reagents

Hexchloroplatinic acid (99.998%) was supplied by Sigma Aldrich. Zinc nitrate hexahydrate ($ZnNo_3{\cdot}6H_2O$, 99%) and hexamethylenetetramine (HMTA, 99%) were purchased from Sinopharm chemical Reagent Co., Ltd. Methanol was obtained from Beijing Modern Eastern Fine chemical and Nafion (5 wt.%) were purchased from Dupont. Other chemicals were of analytical-regent grade without further purification.

2.2. Controlled synthesis of ZnO, Pt and Pt–ZnO nanospheres

The ZnO, Pt and PtZONS were synthesized by the same method as we reported previously [19]. Briefly, for the controlled synthesis of nanospheres, Au coated Si (0 0 1) substrates were used as the working electrode and the products were obtained after 5 min, 10 min and 30 min electrodeposition by a CHI660C electrochemical workstation. The electrolyte was 100 mL aqueous solution containing 0.01 M $H_2PtCl_6{\cdot}(H_2O)_6$, 0.01 M $ZnNO_3$ + 0.01 M HMTA and 0.01 M $ZnNO_3$ + 0.01 M HMTA + 0.01 M $H_2PtCl_6{\cdot}(H_2O)_6$ respectively. The applied voltage was 1 V with a current density 6.043 mA cm^{-2} at room temperature. The as synthesized nanospheres were characterized by scanning electron microscope (SEM-6301F), HRTEM (JEM-2011), EDS and X-ray spectroscopy (XPS).

2.3. Fabrication of modified glassy carbon electrode

To test the methanol sensing capabilities of ZnO, Pt and PtZONS, a conventional glassy carbon electrode (GCE) was modified with nanospheres by the same method as used previously [36]. To prepare the working electrode, 10 mg sample (each case) was dispersed in 900 μL isopropanol + 100 μL Nafion solutions (5 wt.%) and then ultrasonically dispersed for 15 min to form a uniform suspension. Then, 1.0 μL of the suspension was dropped onto a GCE (3 mm in diameter) to form a uniform layer and dried at 60 °C for 20 min. The electrochemical measurements were performed at room temperature with a three electrode configuration in a pH 7 buffer aqueous solution. Platinum was used as the counter electrode with Hg/Hg_2SO_4 as the reference electrode saturated in K_2SO_4.

3. Results and discussion

3.1. Characterization of nanospheres

Fig. 1(a) shows the schematic diagram and illustrates the formation of PtZONS. Fig. 1(b and c) presents a typical FESEM images of the product obtained after 5 min deposition on Si substrate. It can be seen that whole substrate is decorated with individual nanospheres in the shape of fullerene with diameter in the range of 20–250 nm, as clear from diameter vs number of nanospheres (frequency) graph shown in Fig. 1(d). The morphology of the product obtained after 10 min deposition is also shown in Fig. 1(e and f) and demonstrate that the agglomeration of the nanospheres start around the first nanospheres and form a toroidal structure with diameter about 120–400 nm as illustrates in Fig. 1(g). The product after 30 min deposition exhibits a high-density agglomeration of PtZONS with an average diameter in the range of 0.2–3.5 μm as shown in Fig. 1(h–j). The magnified FESEM image of the single agglomerate as shown in the inset (Fig. 1(h)), clearly displays that PtZONS aggregate and assembled into many separate spherical agglomerates on the surface of first spherical agglomerate that serve as substrate for the further agglomeration. It has been found that the morphology of the nanospheres can be controlled and depends upon the deposition time.

Fig. 2(a) presents a TEM image of the synthesized ZnO nanospheres after 30 min deposition and showing formed nanospheres having uniform diameter of about 20–50 nm. The magnified TEM and HRTEM image of the ZnO nanospheres having the hexagonal structure is shown in Fig. 2(b and c). The fringe spacing distance is measured to be 0.245 nm which correspond to the spacing of (1 0 1) plane of wurtzite ZnO. Fig. 2(d and e) presents the Pt nanospheres after 30 min deposition and illustrates the high-density agglomeration of nanospheres. The HRTEM image of individual Pt nanospheres exhibits the polycrystalline nature of the nanospheres as shown in Fig. 2(f). The interplanar distance is also measured to be 0.225 nm corresponds to the spacing of (1 1 1) Pt plane as shown in Fig. 2(f).

In order to further investigate the microstructure of PtZONS 3D assembly, the TEM and HRTEM images have been recorded as shown in Fig. 3(a–e). The TEM images of the self assembled agglomerates and the magnified TEM image of the PtZONS are shown in Fig. 3(a and b). The HRTEM images taken from the doted areas in (Fig. 3(a and b)) are shown in Fig. 3(c–e) and found to be polycrystalline as shown in Fig. 3(c–e). The interplanar distance of fringes is measured to be 0.245 nm and 0.225 nm which correspond to the spacing of (1 0 1) plane of wurtzite ZnO and (1 1 1) Pt plane respectively as shown in Fig. 3(c). The SAED over a dozen of nanospheres is performed as shown in Fig. 3 (d) inset. The arrows in Fig. 3(e) indicate the incorporated Pt nanoparticles into ZnO nanospheres. Fig. 3(f) shows the EDS spectrum taken from the circular doted area in Fig. 3(b). The Pt peaks appear at about 2.12 KeV confirms the presence of Pt nanoparticles in nanospheres. Quantitative analysis reveals that the average amount of pt contents is about 2.5 at.% in each Pt–ZnO nanospheres. Statistical analysis of EDS measurements over dozen of PtZONS demonstrates that the incorporated pt nanoparticles are randomly distributed into the ZnO nanospheres.

The XPS survey spectra of the PtZONS sample is shown in Fig. 4 for the analysis of valence state of the Pt element in PtZONS. The spectrum shows that the Pt peaks are located at 71.3 eV and 74.6 eV corresponding to the electronic states of $Pt4f_{7/2}$ and $Pt4f_{5/2}$ respec-

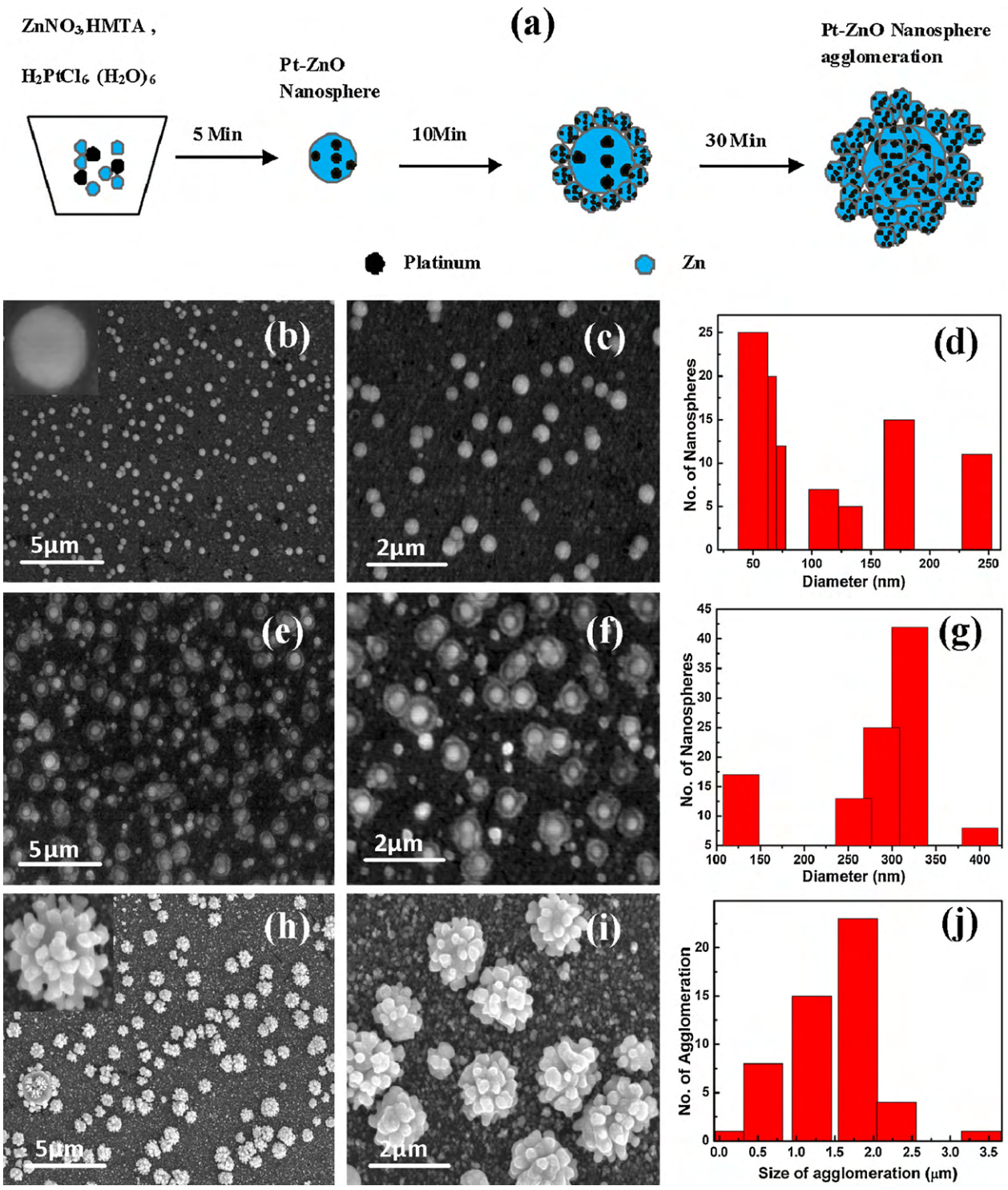

Fig. 1. (a) Schematic diagram of the formation of Pt–ZnO nanospheres. Typical SEM images of Pt–ZnO nanospheres after (b and c) 5 min deposition (e and f) 10 min deposition (h and i) 30 min deposition (d, g and j). Graphs between diameter vs number of nanospheres obtain at 5 min, 10 min and 30 min deposition respectively.

tively as shown in Fig. 4(inset). The energy difference between two peaks is about 3.3 eV which is similar to the reported value [37]. These peaks confirm the presence of metallic platinum, in the nanospheres. On the other hand, XPS spectrum of Zn is also shown in Fig. 4(inset) corresponding to $Zn2p_{3/2}$ and $Zn2p_{1/2}$ peaks. From the peak position it is observed that the Pt binding energy peaks are slightly shifted towards lower binding energy side while Zn peak shift towards higher binding energy side with respect to the reported [38]. These binding energy shifts is due to the Pt-incorporation into ZnO nanospheres. Furthermore, an increase in neutral platinum content of the as deposited PtZONS film is also observed which is similar to the reported previously for Pt:ZnO film (Ref. [11]). It also suggests the successful Pt-incorporation into ZnO lattice because the formation of the Pt–ZnO bond may involve a net charge transfer. The average contents of Pt are consistent with the EDS measurements.

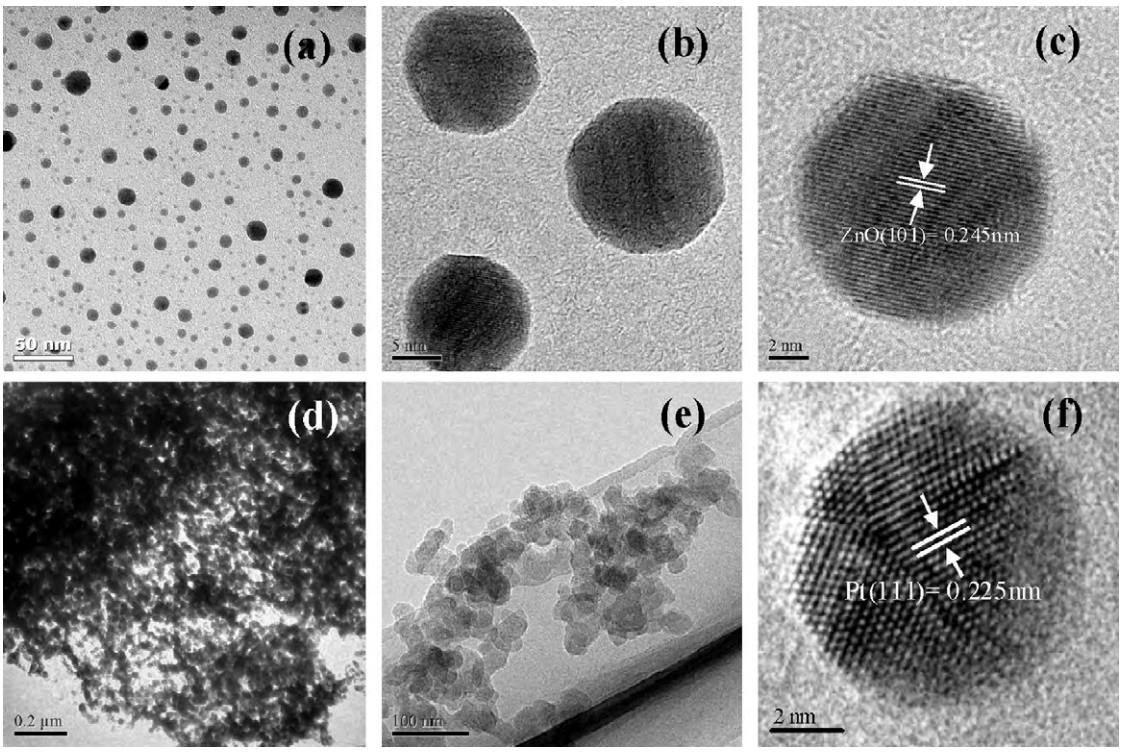

Fig. 2. (a) TEM image of ZnO nanosphere. (b) Magnified TEM image. (c) HRTEM image of the individual nanospheres. (d) TEM image of Pt nanosphere. (e) Magnified TEM image of Pt nanosphere. (f) HRTEM image of individual Pt nanospheres.

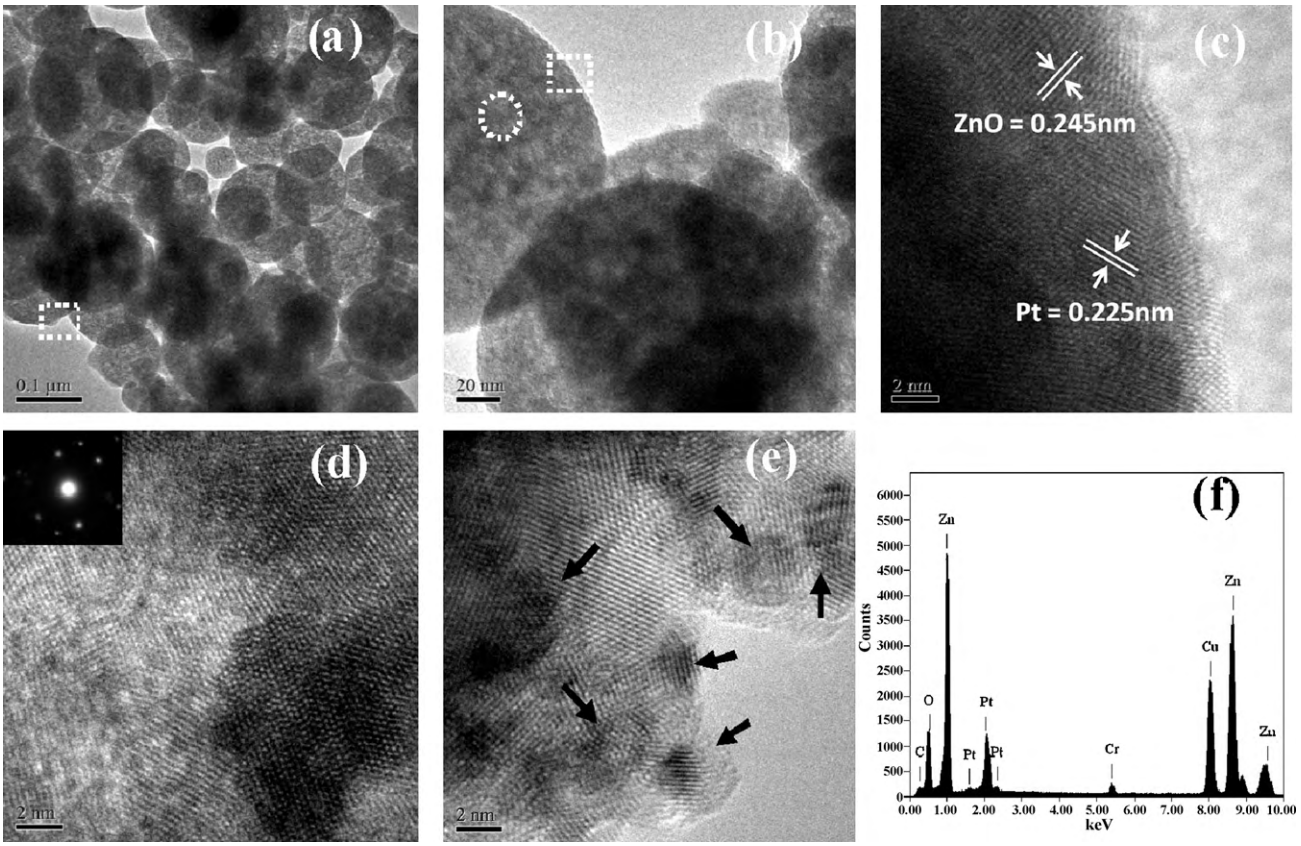

Fig. 3. (a) TEM image of Pt–ZnO nanospheres agglomeration. (b) Magnified TEM image. (c) HRTEM images of the nanosphere from the square doted area in figure (b). (d) HRTEM image of taken from the central part, insets is SAED (e) HRTEM image from square doted area in figure (a). (f) EDS.

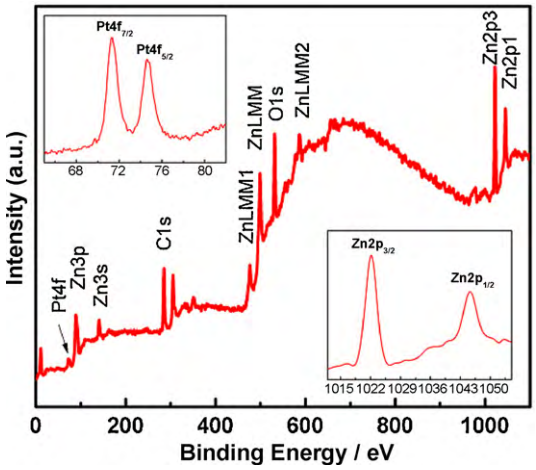

Fig. 4. (a). XPS survey spectrum of the PtZONS (inset top left) Pt4f; (inset bottom right) Zn2p.

3.2. Detection of methanol with Pt–ZnO modified glassy carbon electrode

3.2.1. Cyclic voltammetry

To investigate the electrocatalytic behavior toward the electrochemical reaction of methanol at the PtZONS film, the modified electrode (Nafion/PtZONS/GC) is characterized by a cyclic voltammetry (CV) sweep curve ranging from −0.2 to +0.3 V vs Hg/Hg_2SO_4 at a scan rate of 20 mV/s as can be seen in Fig. 5(a and b). For comparison, CVs with Nafion/ZONS/GC and Nafion/PtNS/GC modified electrodes in the presence of 0.2 M methanol in terms of mass-normalized currents that represent the overall catalytic activities are shown in Fig. 5(a). It can be seen that CV with Nafion/PtZONS/GC modified electrode change significantly with obvious increases of the oxidation current in the range 0.05–0.2 V. This can be attributed to the role of incorporated Pt nanoparticles into ZnO nanospheres which led to enhance the electrocatalytic ability and allow the determination of methanol at a lower working potential. In fact, during the methanol oxidation Pt is poisoned by the intermediate species such as CO and other carbonaceous species HCO or COH. Therefore, the oxidation current by the Pt modified electrode decreases due to the coverage of Pt active sites with the intermediate species as shown in Fig. 5(a). On the other hand, since there is net charge transfer in PtZONS, the Pt catalytic sites would increase because the coverage of CO on the Pt surface reduce due to the decrease Pt–CO binding energy, which ultimately enhance the electrocatalytic activity of PtZONS with respect to that of pure Pt and ZnO. The CV curves in terms of mass-normalized currents corresponding to different morphology of PtZONS are shown in Fig. 5(b). The difference in the CV curves a–c clearly shows the effect of morphology on the methanol oxidation. It can be seen that the CV, a for PtZONS obtained after 30 min deposition (agglomeration) exhibits an increase in oxidation current with respect to the CVs, b and c for morphology obtained at 10 min and 5 min deposition. It demonstrates that as the agglomeration increases, the electrocatalytic activity of the corresponding modified electrode increases, due to the increase number of Pt particles into ZnO nanospheres. Furthermore, this study reveals that the electrocatalytic activity of PtZONS electrode for methanol oxidation is not only dependent on the morphology but also strongly dependent on the distribution of Pt into PtZONS.

3.2.2. Amperometric response

The typical mass-normalized amperometric responses of the three modified electrodes to the successive addition of 0.1 M methanol at +0.5 V vs Hg/Hg_2SO_4 are shown in Fig. 6(a). In comparison with the Nafion/ZONS/GC and Nafion/PtNS/GC modified electrodes, the Nafion/PtZONS/GC modified electrode exhibits a rapid and sensitive response to the change of methanol and an obvious increase in current upon successive addition of 0.1 M methanol as clearly observed in the figure. Fig. 6(b) illustrates an amperometric response of the Nafion/PtZONS/GC modified electrode with different methanol concentration (from 0.01 M to 1.0 M) into continuously stirred 0.1 M phosphate buffer (PB) solution at +0.5 V. It has been revealed that the modified electrode exhibit an obvious increase in current at different methanol concentrations. The modified electrode achieved 95% steady state current within less than 10 s. This indicates a good electro-catalytic oxidative and fast electron exchange behavior of the modified electrode. The low detection limit for the modified electrode toward methanol is 0.01 M as shown in the figure.

3.2.3. Temperature effect

The calibration curves of the modified electrode with increasing concentration at various temperatures are shown in Fig. 6(c). Following the increase of the methanol concentration, the response current increases linearly from 0.01 M to 1.0 M (correction coefficient $R = 0.9768$) at room temperature (25 °C) and starts saturation at high concentration of methanol which suggest the saturation of active sites of the electrode at those methanol levels. It has been revealed that at temperatures (40 °C, 50 °C and 60 °C) the response current increases linearly with the increase of methanol concentration which suggests that electrocatalytic

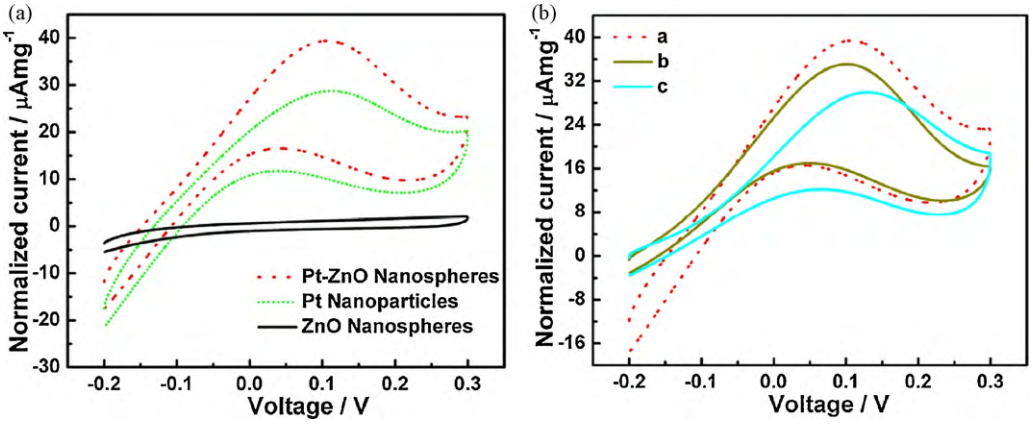

Fig. 5. (a). Cyclic voltammograms of ZnO, Pt and Pt–ZnO modified GCE in the presence of 0.2 M methanol in pH 7.0 PB solution at a scanning rate of 20 mV s^{-1}. (b) Cyclic voltammograms of different morphology Pt–ZnO modified GCE in the presence of 0.2 M methanol. The currents are normalized to the mass of Pt.

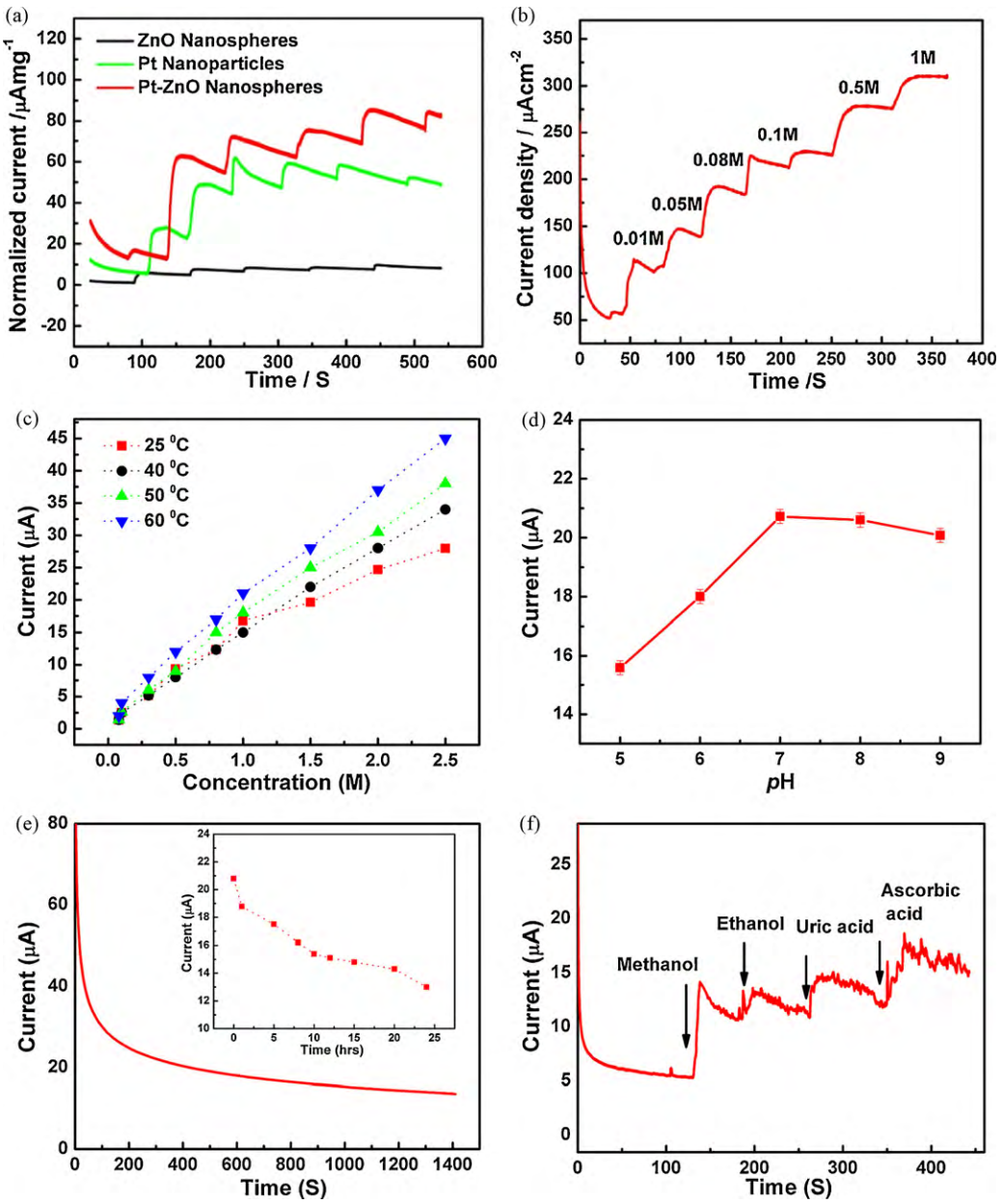

Fig. 6. (a) Mass-normalized amperometric response of three modified GC electrodes at +0.5 V with successive increase in 0.1 M methanol concentration. (b) Amperometric response of Pt–ZnO modified GC electrode with different concentrations of methanol at +0.5 V. (c) Calibrated curves of the modified electrode with increase in methanol concentration at various temperatures. (d) Amperometric response of the modified GC electrode in PB solution with increasing pH containing 0.1 M methanol. (e) Long-term stability of the modified electrode. (f) Amperometric response of the modified GC electrode for the successive addition of electroactive species.

activity of the modified electrode is more stable at higher temperatures. The excellent thermoresistance of the modified electrode is ascribed to the PtZONS film that greatly enhances the thermal stability of the sensor. The sensitivity of the modified electrode is achieved about 235.47 $\mu A\,M^{-1}\,cm^{-2}$ which is much higher than the Nafion/ZONS/GC and Nafion/PtNS/GC modified electrodes. These results prove that PtZONS used as matrix increase the electrocatalytic activity which in turn enhances the sensitivity of the modified electrode to methanol detection.

3.2.4. pH response

The activity of the modified electrode is also affected by the pH of the PB solution therefore; the pH effect on the modified electrode performance is also investigated by measuring the current response to 0.1 M methanol at +0.5 V. As the ZnO is a kind of amphoteric compound and not stable in both strong acid and base solutions, the pH dependence of the sensor is evaluated in the range of pH 5–9 in this experiment. As clearly seen in Fig. 6(d) the sensor shows an optimal sensitivity of response at pH 7.1 corresponding to a series of pH value.

3.2.5. Long-term stability

Fig. 6(e) shows the amperometric response of the methanol sensing electrode in the presence of 0.1 M methanol at a scanning rate of 20 mV s^{-1}. It is clearly observed that the electrode exhibits good stability with a loss of 3% activity after 20 min. The long-term stability of the electrode is also examined by determining performance after every 3 h as shown in the inset Fig. 6(e). Although the electrode responses gradually decreases but it retains about 94% of

Table 1
Performance characteristics of the Nafion/PtZONS/GC modified electrode.

Sensitivity ($\mu A\,M^{-1}\,cm^{-2}$)	235.47
Linear range (M)	0.03–1
Response time (s)	<10
Detection limit (M)	0.03
Appl. potential (V)	0.5

its original response after 24 h. This shows that the electrode has good stability for the methanol detection.

3.2.6. Selectivity

The influence of some electroactive species on the performance of the electrode is also examined as shown in Fig. 6(f). The amperometric response of the electrode after the addition of methanol, ethanol, uric acid and ascorbic acid is determined as shown in the figure. The concentration of the added species is 0.05 M for methanol and 0.1 M for the others. It can be seen that electrode response time is less than 10 s for methanol. Although the addition of alcohol, uric acid and ascorbic acid bring a small increase in current, indicating that these species interfere slightly in the measurement of methanol. However, the response of each species is very small, compare to the methanol response. These results demonstrate that the modified electrode has good anti-interference ability for the determination of methanol.

3.2.7. Performance of the electrode

At the optimized conditions, the detection limit, linear range and sensitivity of the modified electrode to methanol are determined and are listed in Table 1. From the characteristics, it is confirmed that the presented modified electrode exhibit an excellent performance.

4. Conclusions

In conclusion, Pt-incorporated ZnO based hybrid nanospheres have been successfully synthesized by controlled electrodeposition. It has been found that the morphology of the nanospheres can be controlled and depends upon the deposition time. The electrochemical measurements show that the PtZONS possess superb active surface area and high catalytic activity for methanol electrooxidation. A reproducible sensitivity of 235.47 $\mu A\,M^{-1}\,cm^{-2}$ within a response time less than 10 s has been achieved with PtZONS modified GCE. It has been revealed that ZnO improve the electrocatalytic activity of Pt nanoparticles, which in turn enhance the sensitivity of the electrode for methanol detection. Hence, PtZONS provide a new platform for the fabrication of nanosensors that could be useful for monitor the concentration of methanol fuel used in direct methanol fuel cells and biological processes.

Acknowledgment

This work is financially supported by National 973 Project of China and Chinese National Nature Science Foundation. This work made use of the resources of the Beijing National Center for Electron Microscopy. The authors are also grateful to the Higher Education Commission (HEC) and PINSTECH (PAEC) Pakistan for the financial support to Mashkoor Ahmad.

References

[1] D.J. Milliron, S.M. Hughes, Y. Cui, L. Manna, J.B. Li, L.W. Wang, A.P. Alivisatos, Nature 430 (2004) 190.
[2] E. Elmalem, A.E. Saunders, R. Costi, A. Salant, U. Banin, Adv. Mater. 20 (2008) 3739.
[3] J. Liu, W. Chen, X. Liu, K. Zhou, Y. Li, Nano Res. 1 (2008) 46.
[4] H. Zeng, J. Li, J.P. Liu, Z.L. Wang, S.H. Sun, Nature 420 (2002) 395.
[5] Y.Q. Li, G. Zhang, A.V. Nurmikko, S.H. Sun, Nano Lett. 5 (2005) 1689.
[6] H. Kim, M. Achermann, L.P. Balet, J.A. Hollingsworth, V.I. Klimov, J. Am. Chem. Soc. 127 (2005) 544.
[7] W.L. Shi, Y. Sahoo, H. Zeng, Y. Ding, Z.L. Wang, M.T. Swihart, P.N. Prasad, Adv. Mater. 18 (2006) 1889.
[8] M. Yamada, S. Kon, M. Yiyake, Chem. Lett. 34 (2004) 1050.
[9] T. Teranishi, M. Hosoe, T. Tanaka, M. Miyake, J. Phys. Chem. B 103 (1999) 3818.
[10] M.A. El-Sayed, Acc. Chem. Res. 34 (2001) 257.
[11] J.E. Gregory, R. Aimee, Q.W. Li, F.W. Charles Jr., J. Vac. Sci. Technol. A 16 (1998) 1926.
[12] S.H. Sun, C.B. Murray, D. Weller, L. Folks, A. Moser, Science 287 (2000) 1989.
[13] S.H. Sun, Adv. Mater. 18 (2006) 393.
[14] Z.W. Pan, Z.R. Dai, Z.L. Wang, Science 291 (2001) 1947.
[15] R.F. Service, Science 276 (1997) 895.
[16] W.L. Wang, Mater. Today 7 (2004) 26.
[17] M. Ahmad, C. Pan, J. Iqbal, L. Gan, J. Zhu, Chem. Phys. Lett. 480 (2009) 105.
[18] J.X. Wang, X.W. Sun, A. Wei, Y. Lei, X.P. Cai, C.M. Li, Z.L. Dong, Appl. Phys. Lett. 88 (2006) 233106.
[19] M. Ahmad, C. Pan, L. Gan, Z. Nawaz, J. Zhu, J. Phys. Chem. C 114 (2010) 243.
[20] N.D. Brinkman, E.E. Ecklund, R.J. Nichols, Fuel Methanol: A Decade of Progress, Society of Automotive Engineers, Warrendale, PA, 1990.
[21] Methanol toxicity [microfilm], in: US Department of Health & Human Services, Public Health Service, Agency for Toxic Substances and Disease Registry, Atlanta, GA, 1992.
[22] P.A. de Paula Pereira, E.T. Sousa Santos, T. de Freitas Ferreira, J.B. de Andrade, Talanta 49 (1999) 245.
[23] X.P. Lee, T. Kumazawa, K. Kondo, K. Sato, O. Suzuki, J. Chromatogr. B 734 (1999) 155.
[24] J.F. Livesey, S.L. Perkins, N.E. Tokessy, M.J. Maddock, Clin. Chem. 41 (1995) 300.
[25] F. Tagliaro, G. Schiavon, R. Dorizzi, M. Marigo, J. Chromatogr. Biomed. Appl. 563 (1991) 11.
[26] A.I. HajYehia, L.Z. Benet, J. Chromatogr. A 724 (1996) 107.
[27] S.H. Chen, H.L. Wu, C.H. Yen, S.M. Wu, S.J. Lin, H.S. Kou, J. Chromatogr. A 799 (1998) 93.
[28] J.M. Garrigues, A. Perez-Ponce, S. Garrigues, M. de la Guardia, Vib. Spectrosc. 15 (1997) 219.
[29] R. Parsons, T. VanderNoot, J. Elcctroanal. Chem. 257 (1988) 9.
[30] S.G. Sun, J. Clavilier, J. Electroanal. Chem. 236 (1987) 95.
[31] T. iwasita, F.C. Nart, N. Lopez, W. Vielstich, Electrochim. Acta 37 (1992) 2361.
[32] T. Iwasita, W. Vielstich, E. Santos, J. Electroanal. Chem. 229 (1987) 367.
[33] S. Wilhehn, T. Iwasita, W. Vielstich, J. Electroanal. Chem. 238 (1987) 383.
[34] B. Bittins-Cattaneo, E. Cattanco, P.I. K6nigshovcn, W. Vielstich, in: A.J. Bard (Ed.), Electroanalylical Chemistry, vol. 17, Marcel-Dekker, New York, 1991, p. 181.
[35] B. Beden, J.M. Leger, C. Lamy, in: J.O'M. Bockris, B.E. Conway, R.E. White (Eds.), Modern Aspects of Electrochemistry, vol. 22, Plenum Press, New York, 1992, p. 97.
[36] M. Ahmad, C. Pan, J. Zhu, J. Mater. Chem. (2010), doi:10.1039/C0JM01055C.
[37] K.X. Yao, H.C. Zeng, Langmuir 24 (2008) 14234.
[38] B. Christina, P. Chantal, C. Martin, A.B. Gianluigi, R.M. Barry, J. Am. Chem. Soc. 126 (2004) 8028.